Am J Clin Exp Urol 2020;8(1):48-58
www.ajceu.us /ISSN:2330-1910/AJCEU0108709

Original Article

Transcriptional profiling of tumor associated macrophages in human renal cell carcinoma reveals significant heterogeneity and opportunity for immunomodulation

Thomas R Nirschl[1,2,3*], Margueritta El Asmar[2,3,4*], Wesley W Ludwig[5*], Sudipto Ganguly[2,3], Michael A Gorin[5], Michael H Johnson[5], Phillip M Pierorazio[5], Charles G Drake[2,6], Mohamad E Allaf[5], Jelani C Zarif[2,3]

[1]Pathobiology Graduate Program, Johns Hopkins University School of Medicine, Baltimore, MD 21287, USA; [2]Bloomberg~Kimmel Institute for Cancer Immunotherapy, [3]Department of Oncology, Johns Hopkins School of Medicine and The Sidney Kimmel Comprehensive Cancer Center, Baltimore, MD 21231, USA; [4]Department of Medicine, Johns Hopkins University, Baltimore, MD 21287, USA; [5]The James Buchanan Brady Urological Institute at the Johns Hopkins University School of Medicine Baltimore, MD 21287, USA; [6]Department of Medicine, New York-Presbyterian/Columbia University Medical Center (CUMC), New York City, NY 10027, USA. [*]Equal contributors.

Received February 4, 2020; Accepted February 18, 2020; Epub February 25, 2020; Published February 28, 2020

Abstract: Among the more notable immunotherapies are checkpoint inhibitors, which prevent suppressive signaling on T cells, thereby (re)activating them to kill tumor cells. Despite remarkable treatment responses to immune checkpoint blockade, with a subset of patients achieving complete responses, a large population have little-to-no response, dictating the necessity of further research in this field. Myeloid derived cells heavily infiltrate the tumor microenvironment (TME) of many cancers and are believed to have a number of potent anti-inflammatory effects. Here we use primary non-metastatic renal cell carcinoma to interrogate the gene expression profiles of M2-tumor associated macrophages (M2-TAMs). We performed Fluorescent Activated Cell (FACS) sorting on monocytes from the peripheral blood and tumors of fresh clear cell renal cell carcinoma (ccRCC) samples obtained after patients underwent a partial (7 patients-87.5%) or radical (1 patient-12.5%) nephrectomy. We then utilized NanoString gene expression profiling to show that TAMs express a heterogeneous transcriptional profile that does not cleanly fit into the traditional M1-M2 TAM paradigm. We identified expression of M1 associated costimulatory molecules, a multitude of diverse chemokines, canonical M2 associated molecules, as well as factors involved in the Complement system and checkpoint receptors. Our data are in agreement with other published literature investigating TAMs in various non-ccRCC TMEs, and support the growing literature concerning expression of Complement factors and checkpoint receptors on TAMs.

Keywords: Renal cell carcinoma (RCC), M2-tumor-associated macrophages (TAMs), M1-TAMs, M2-TAMs, transcriptional profiling

Introduction

Renal cell carcinoma (RCC) is a common cancer in the United States with nearly 64,000 newly diagnosed cases each year which encompasses several distinct subtypes, with clear cell renal cell carcinoma (ccRCC) being the most abundant [1]. While a partial or radical nephrectomy for non-metastatic disease has a favorable 5-year survival rate, approximately one quarter of patients (25%) diagnosed with RCC already have metastatic disease [2]. Additionally, RCC is often inherently resistant to chemotherapy and radiotherapy [3], and as such, there is a critical need to develop new therapies which are capable of treating both metastatic and localized disease.

Immunotherapy offers a unique and potent approach to cancer treatment by harnessing the patient's immune system to control and even eliminate tumors. While there are many

approaches to enhancing the patients' endogenous anti-tumor responses, immune checkpoint inhibitors have risen as a clear leader in the field. Mechanistically, immunotherapy treatments can promote tumor infiltration and cytolytic activity by T cells by blocking key inhibitory receptors or ligands (CTLA-4, PD-1, LAG-3, TIM-3, PD-L1, PD-L2), and are able to elicit potent and durable antitumor responses in subsets of patients treated with both single agents and combination therapies across several cancer types [4-7]. Despite this, not all patients will respond to checkpoint blockade therapy indicating that there must be additional factors in the tumor microenvironment (TME) limiting inflammation and therefore reducing the efficacy of immunotherapies.

One such mechanism of immunosuppression in the TME are M2-tumor associated macrophages (M2-TAMs). M2-TAMs have a variety of suppressive mechanisms including expressing inhibitory ligands, depleting critical nutrients in the TME, as well as secreting suppressive cytokines such as TGF-β and IL-10 [8-10]. Despite this, there is much left unknown concerning other aspects of these cells in localized renal cell carcinoma, and which molecules should be modulated to specifically reduce their immune suppressive functions, increase the efficacy of other therapies or even potentially induce a potent anti-cancer inflammatory response. Many cancers, including RCC is heavily infiltrated by myeloid cells even in localized early stage disease [9, 11], indicating that these cells are likely playing a role in early tumor progression. Herein, we set out to determine the transcriptional profiles of M2-TAMs in ccRCC that may reveal new potential therapeutic targets to improve patient outcomes.

Materials and methods

Patient samples

Eight patients undergoing either a partial (7) or radical (1) nephrectomy were consented under the approved protocol number (IRB00033839) by the Johns Hopkins Internal Review board (IRB). Four patients were of African-American descent (50%) and four patients were of Caucasian descent (50%). These patients were treatment naïve, as such that these patients had not undergone any previous treatment for their disease prior to surgery. At the time of surgery, 30 mL of matched patient whole blood was obtained in heparinized syringes to prevent clotting. The sample was sent straight from the operating room to surgical pathology, where the diagnosis was confirmed and a sample was obtained for research purposes within hours of surgery.

Whole blood processing

Whole blood was obtained pre-surgery in heparinized syringes to prevent clotting. 15 mL of whole blood was aliquoted per 50 ml conical tube (Falcon, Cat # 352098), with 20 mL of 1X PBS (Quality Biological, Cat # 114-058-101) added to each tube, and finally an additional 15 mL underlay of Ficoll-Paque PLUS density gradient media (GE Healthcare Life Sciences, Cat # 17144003) for a total volume of 50 mL. Samples were centrifuged at 2000 rpm (845 rcf) for 25 minutes at room temperature and allowed to stop without breaks. Peripheral blood mononuclear cells (PBMCs) were isolated and combined into a single 50 mL tube and washed in 1X PBS prior to being counted on a hemocytometer. Samples were resuspended in 50 ml of complete media (cMedia = RPMI 1640 + 10% FBS + 1% MEM Nonessential Amino Acids + 1% Glutamine + 1% Pen/Strep) and stored on a rocking unit at room temperature until downstream application.

Tissue processing

Fresh tissue was digested using the Human Tumor Dissociation Kit (Miltenyi Biotec, Cat # 130-095-929) and the gentleMACS Octo Dissociator (Miltenyi Biotec, Cat # 130-096-427). The resulting single cell suspension was passed through a 100 uM cell strainer and washed with 1X PBS, after which it was resuspended in cMedia.

Flow cytometry and flow sorting

Both PBMCs and TME samples were washed in 1X PBS, spun down at 1300 RPM for 10 minutes and then resuspended in 1X PBS and plated into a 96-well u-bottom plate respectively. Samples were stained for viability using LIVE/DEAD Fixable Aqua Dead Cell Stain Kit (ThermoFisher Scientific, Cat # L34957) at a dilution of 1:1000 for 30 minutes at room temperature in the dark. Cells were then brought up to a final volume of 200 uL with PBS, spun down

and resuspended in 100 uL of an antibody mastermix containing the following surface markers; CD45-APC-Cy7 1:10 (BD Biosciences, Cat # 557833), CD3-AF700 1:20 (BD Biosciences, Cat # 557943), CD11b-FITC 1:20 (BD Biosciences, Cat # 562793), CD11c-PE-Cy7 1:50 (BD Biosciences, Cat # 557833), CD14-PerCP-Cy5.5 1:50 (BD Biosciences, Cat # 561356), CD33-APC 1:50 (BD Biosciences, Cat # 557918), HLA-DR-BV605 1:10 (BD Biosciences, Cat # 560359), and CD15-PE (Biolegend, Cat# 301906). Cells were washed in 1X PBS and sorted on the BD FACSARIA II flow cytometer. They were then FACS sorted directly into 1.7 mL tubes containing 800 uL of Trizol LS (ThermoFisher Scientific, Cat # 10296028), and stored at -80°C until RNA isolation. Data was analyzed using FlowJo Software (Tree Star, Mac version 9.9.4).

RNA isolation

Trizol tubes were allowed to thaw at room temperature for ~10 minutes. Exactly 160 µL of chloroform was then added to each tube which were then mixed by inversion for 15 seconds each. Samples were centrifuged at maximum speed for 20 minutes at 4°C. The chloroform layer was carefully removed and transferred to a new, RNAse free 1.7 mL tube (Thomas Scientific, Cat # C2170), with extreme care being taken not to disturb the Trizol layer. Once completed, 400 uL of 100% isopropanol and 2 µL of molecular grade glycogen (ThermoFisher Scientific, Cat # R0561) were then added to each sample respectively. Samples were mixed by inversion for 15 seconds, and allowed to incubate at room temperature for 10 minutes. Samples were centrifuged for 10 minutes at full speed at 4°C. Supernatant was removed and discarded with care not to disturb the glycogen pellet. The pellet was then washed with 70% EtOH, dislodging the pellet from the tube, but not attempting to resuspend it. Samples were then centrifuged at full speed at 4°C for 10 minutes. Supernatant was removed and discarded, and the remaining 70% EtOH was allowed to evaporate at room temperature for 15 minutes. The pellet was then resuspended in 10 µL of RNAse/DNAse free molecular grade water, and tested via bioanalyzer for RNA quality.

Amplification and Nanostring

RNA samples underwent cDNA conversion and subsequent amplification using the NuGEN Ovation Pico WTA System V2 which has an input range of 500 pg to 50 ng (NuGEN Technologies, Cat # 3302-12). In brief: total RNA is converted to cDNA, after which amplification is initiated at the 3' ends, as well as at random sites throughout the transcriptome. This allows amplification of both high quality and degraded RNA samples.

The cDNA samples were analyzed using the nCounter PanCancer Immune Profiling Panel (NanoString Technologies, Seattle, WA, USA), which measured the expression of 770 immunologically relevant genes. Briefly; cDNA samples were hybridized overnight to barcoded gene specific probes, after which hybridized cDNA/Probe complexes were processed by the NanoString Prep Station and bound to the nCounter Cartridge, and finally the cDNA/Probe complexes were oriented on the cartridge and imaged by the nCounter Digital Analyzer for barcode identification of transcripts. Samples were run at the SKCCC Immune Monitoring Core facility. Data files were analyzed using the nSolver software, version 4.0 and R v.3.3.2 for the Advanced analysis 2.0. To correct for background levels and prevent artificially high fold-change results, a background threshold was applied to substitute all raw counts at or below threshold to the threshold value of 100 counts. The geometric mean of 6 housekeeping genes provided by the company panel was calculated and used to normalize expression values. Due to irreconcilable quality control issues during data analysis, the sample 3 PBMC monocyte data was not included during these analyses.

Results

Circulating monocytes and ccRCC infiltrating macrophages have distinct transcriptional profiles

To investigate the transcriptional profiles of Clear Cell Renal Cell Carcinoma (ccRCC) patient matched FACS sorted peripheral blood monocytes and Tumor Associated Macrophages (TAMs) were analyzed using NanoString nCounter PanCancer Immune Profiling Panel (**Figure 1**). Using unsupervised gene and sample clustering, we generated a heatmap of the global data set. As expected, the unsupervised clustering resulted in distinct separation of peripheral blood monocytes samples from TAM samples, indicating expression of different

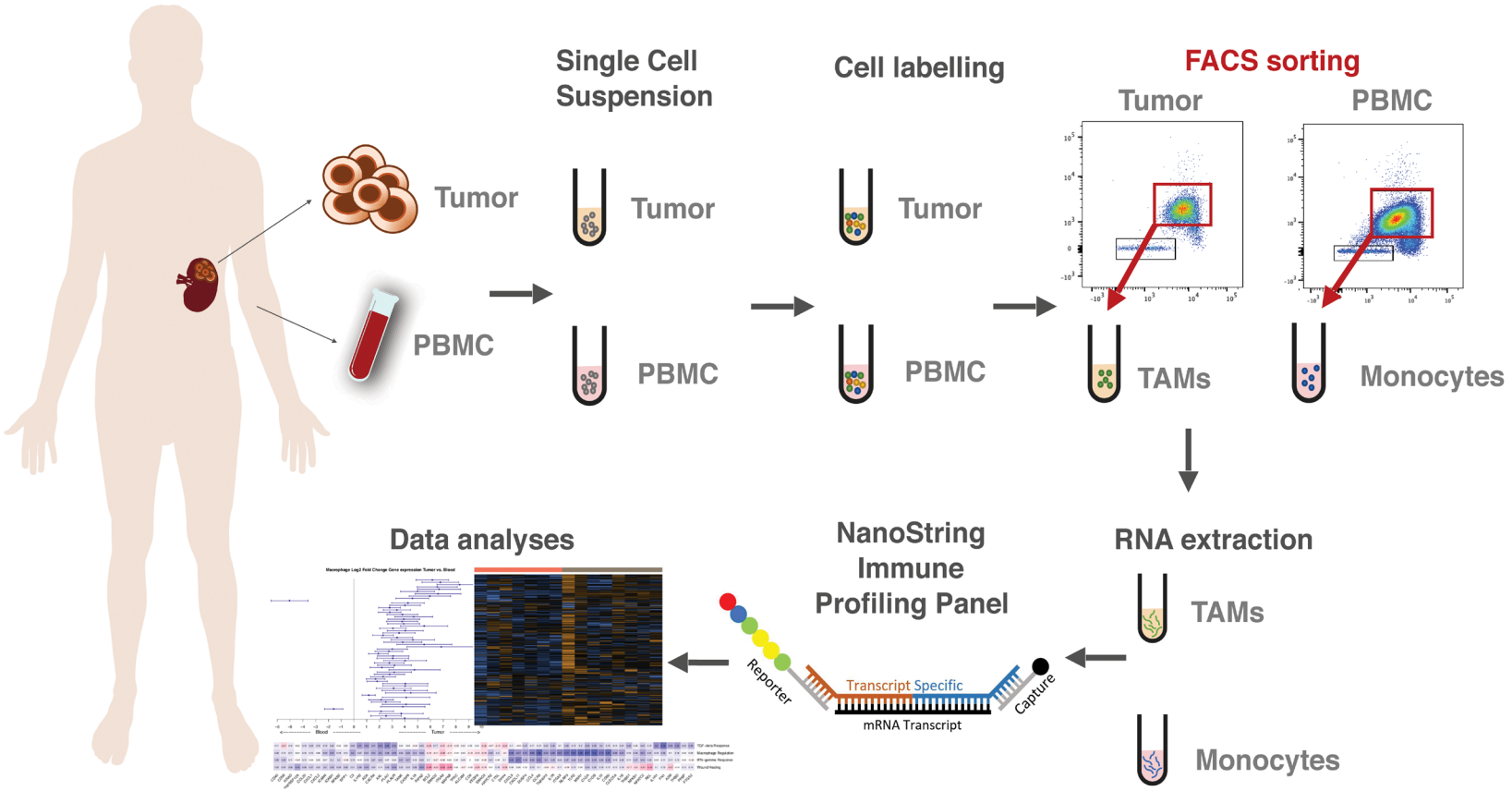

Figure 1. Monocytes and TAMs can be effectively isolated from patient matched whole blood and nephrectomy samples. Whole blood and tumor tissue were obtained upon patient nephrectomy and processed by Ficoll-Paque Plus density centrifugation to obtain PBMCs or enzymatic digestions to obtain whole TME single cell suspensions respectively. The single cell suspensions were then labeled with fluorophore tagged antibodies and underwent FACS to isolate pure Monocyte and Macrophage populations. RNA was extracted from the Monocyte and Macrophage populations, amplified, and analyzed by using the NanoString Pan Immune Profiling panel.

transcriptional profiles in these myeloid populations (**Figure 2A**). We then further characterized those differences using Nanostring pathways analysis (**Figure 2B**). As expected, we found that macrophages isolated from the tumor had a higher adhesion score on average than their counterparts in circulation (P<0.001). Similarly, chemokine (P<0.001), cytokine (P<0.001) and interleukin (P=0.004) gene expression scores were upregulated in tumor, indicating a phenotype characterized by more active inter-cellular signaling. Other scores that were also increased included those of cell cycle (P<0.001), cell function (P<0.001), macrophage functions (P<0.001), pathogen defense (P=0.009), regulation (P<0.001), senescence (P<0.001) and the TNF superfamily (P<0.001). Interestingly, we observed no difference in expression scores associated with antigen processing (P=0.867), cytotoxicity (P=0.232), TLR (P=0.094) or transporter functions (P=0.463) (Supplementary Table 1).

Monocyte and TAM differentially expressed genes can be classified within six broad groups

We identified specific genes that are differentially expressed between the two subsites; 61 genes met statistical significance (**Figure 3A**, **3B**; Supplementary Table 2). Upon closer examination of the data, we excluded TNFRSF12A and DPP4 from interpretation as their expression levels were below threshold in 14/15 samples and significance was being skewed by a single highly expressing sample. We then broadly classified the remaining genes into six groups: adhesion, cytokines/chemokines, inhibitors, surface receptors, transcription factors and a miscellaneous group for the remaining genes which did not fit a distinct group or pattern (Supplementary Figure 1). All identified genes were upregulated in tumor compared to blood, with the exception of PPBP, encoding pro-platelet basic protein (CXCL7), and CASP8, encoding caspase 8, which were significantly downregulated.

TAMs express increased levels of cell adhesion molecules

Among the upregulated adhesion molecules, ALCAM, ICAM-1, ICAM-4, CD58 (LFA-3), CLEC5A (C-type lectin), CD9, ITGA6, and ITGAX (CD11c) are known to be expressed by macrophages and play a role in cell-cell adhesion and/or adhesion to the extracellular matrix (ECM). Among the ECM components, gene expression of FN1 (fibronectin) and THBS1 (thrombospondin I) were also upregulated in tumor compared to blood. Other genes encoding secreted proteins included A2M, a proteinase inhibitor, and PLAU (urokinase). PLAUR, encoding urokinase plasminogen activator receptor, which in addition to ECM remodeling, has been reported to regulate macrophage adhesion and migration through ECM interaction was similarly upregulated [12]. Altogether, these results likely result in enhanced interaction within the ccRCC TME.

TAMs express a multitude of surface receptors, indicating heterogeneous function

We then assessed differential expression of additional surface molecules with non-adhesive functions. In the TAM group, there was increased expression of costimulatory CD40 and CD80 molecules, which mediate activation/proinflammatory signaling in antigen presenting cells (APCs) and T cells respectively. There was also upregulated expression of AXL (AXL Receptor Tyrosine Kinase) which when dimerized by ligand binding results in downstream activation of the PI3K pathway. Additionally, there was increased expression of molecules which have been associated with an M2-TAM phenotype; the scavenger receptor MSR1 (CD204) and the iron uptake receptor TFRC. We found increased expression of the inhibitory receptor HAVCR2 (TIM3) which is commonly discussed in the context of lymphocytes but has been reported on suppressive myeloid cells too [13]. We also observed an increased expression of the innate immune system pathogen recognition receptor, TLR2, and THBD (CD141), which has been described on dendritic and other myeloid cells.

TAMs express both pro and anti-inflammatory cytokines and chemokines

We then examined differentially expressed cytokines and chemokines. As expected, there was upregulation of both pro and anti-inflammatory molecules. Among the pro-inflammatory interleukins upregulated were IL-1B and IL-18. We also noted upregulation in chemokines involved in proinflammatory cell recruitment such as, CXCL2, CXCL9, CXCL11, CCL4 (MIP1B), CCL20 (MIP3A). Conversely, the immu-

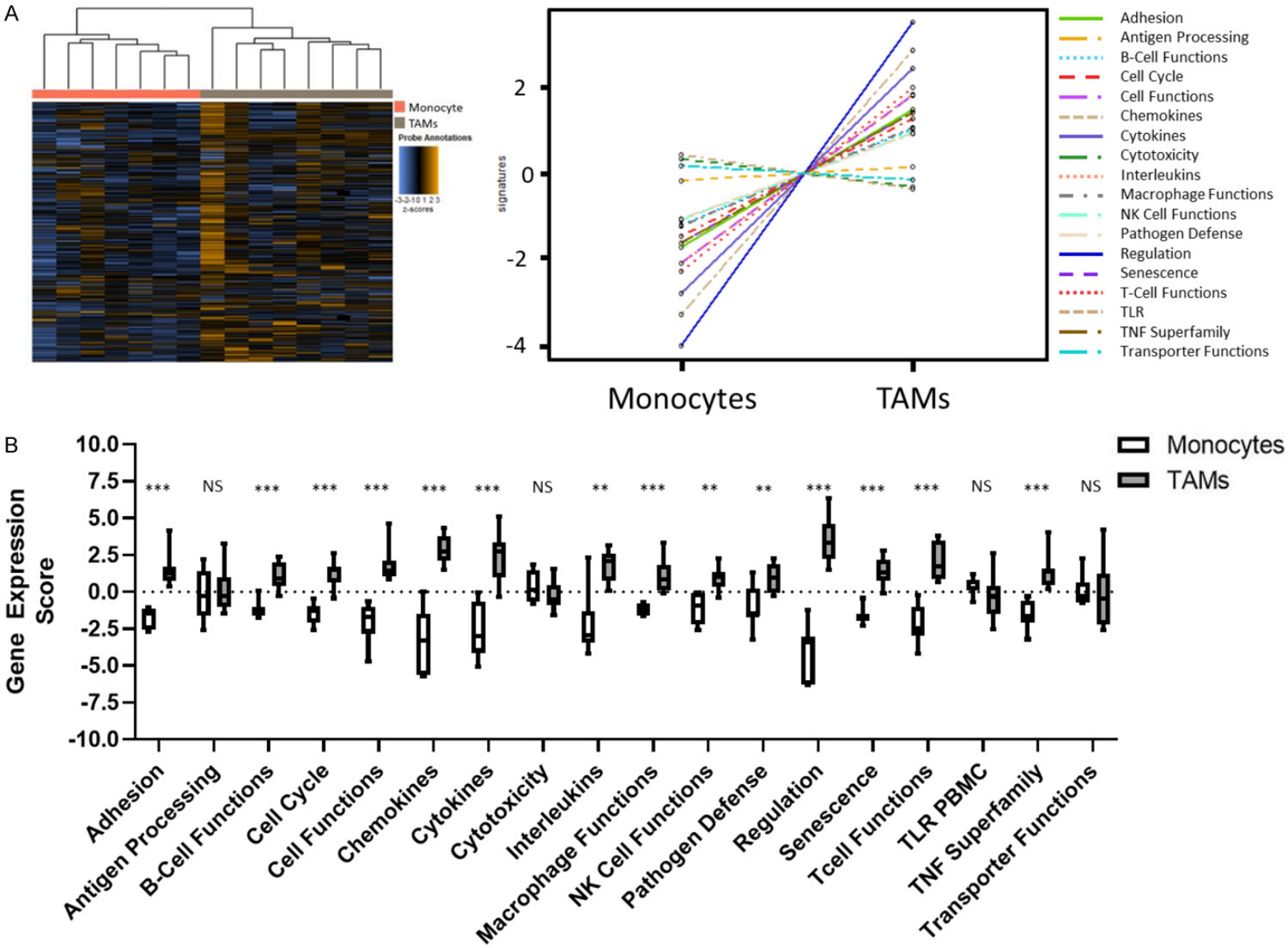
A
Monocyte
TAMs
Probe Annotations
-3-2-10123
z-scores
signatures
2
0
-2
-4
Monocytes
TAMs
Adhesion
Antigen Processing
B-Cell Functions
Cell Cycle
Cell Functions
Chemokines
Cytokines
Cytotoxicity
Interleukins
Macrophage Functions
NK Cell Functions
Pathogen Defense
Regulation
Senescence
T-Cell Functions
TLR
TNF Superfamily
Transporter Functions
B
Gene Expression Score
10.0
7.5
5.0
2.5
0.0
-2.5
-5.0
-7.5
-10.0
Monocytes
TAMs
*** NS *** *** *** *** *** NS ** *** ** ** *** *** *** NS *** NS
Adhesion
Antigen Processing
B-Cell Functions
Cell Cycle
Cell Functions
Chemokines
Cytokines
Cytotoxicity
Interleukins
Macrophage Functions
NK Cell Functions
Pathogen Defense
Regulation
Senescence
Tcell Functions
TLR PBMC
TNF Superfamily
Transporter Functions

Figure 2. Using unsupervised clustering and differentially expressed pathways, monocyte and macrophage populations display unique transcriptional signatures. Monocyte and Macrophage populations were allowed to cluster in an unsupervised manner (A). NanoString Advanced Analysis graphical display of pathway scores. Boxplot representation of pathway scores with significance [P>0.05 = Not Significant (NS), P<0.05 = *, P<0.01 = **, P<0.001 = ***, P<0.0001 = ****] (B).

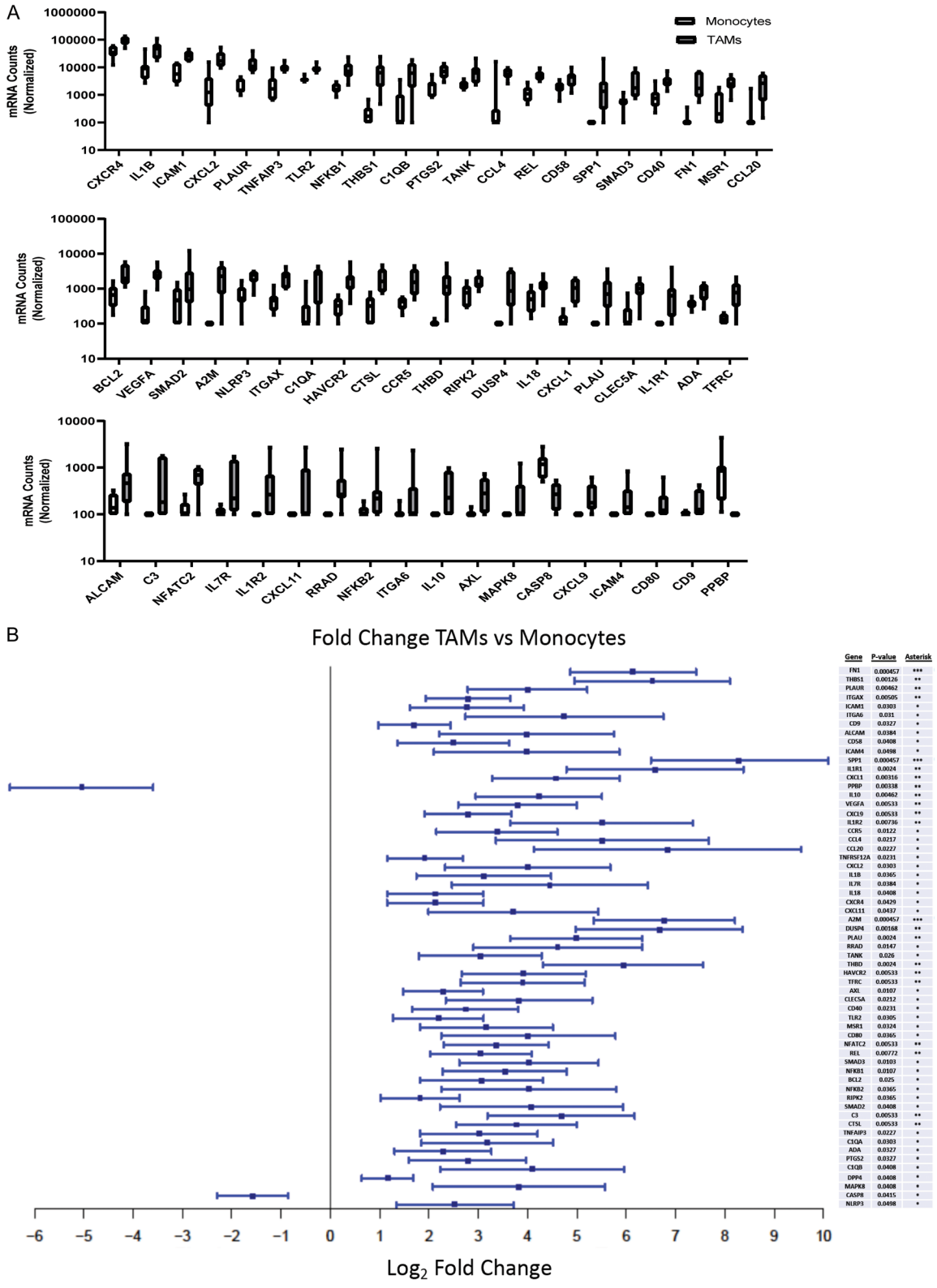

Gene	P-value	Asterisk
FN1	0.000457	***
THBS1	0.00126	**
PLAUR	0.00462	**
ITGAX	0.00505	**
ICAM1	0.0303	*
ITGA6	0.031	*
CD9	0.0327	*
ALCAM	0.0384	*
CD58	0.0408	*
ICAM4	0.0498	*
SPP1	0.000457	***
IL1R1	0.0024	**
CXCL1	0.00316	**
PPBP	0.00338	**
IL10	0.00462	**
VEGFA	0.00533	**
CXCL9	0.00533	**
IL1R2	0.00736	**
CCR5	0.0122	*
CCL4	0.0217	*
CCL20	0.0227	*
TNFRSF12A	0.0231	*
CXCL2	0.0303	*
IL1B	0.0365	*
IL7R	0.0384	*
IL18	0.0408	*
CXCR4	0.0429	*
CXCL11	0.0437	*
A2M	0.000457	***
DUSP4	0.00168	**
PLAU	0.0024	**
RRAD	0.0147	*
TANK	0.026	*
THBD	0.0024	**
HAVCR2	0.00533	**
TFRC	0.00533	**
AXL	0.0107	*
CLEC5A	0.0212	*
CD40	0.0231	*
TLR2	0.0305	*
MSR1	0.0324	*
CD80	0.0365	*
NFATC2	0.00533	**
REL	0.00772	**
SMAD3	0.0103	*
NFKB1	0.0107	*
BCL2	0.025	*
NFKB2	0.0365	*
RIPK2	0.0365	*
SMAD2	0.0408	*
C3	0.00533	**
CTSL	0.00533	**
TNFAIP3	0.0227	*
C1QA	0.0303	*
ADA	0.0327	*
PTGS2	0.0327	*
C1QB	0.0408	*
DPP4	0.0408	*
MAPK8	0.0408	*
CASP8	0.0415	*
NLRP3	0.0498	*

Figure 3. Macrophages isolated from RCC express a heterogeneous set of differentially expressed genes. Monocyte (N=7) and Macrophage (N=8) absolute probe counts for differentially expressed genes (A). Monocyte (N=7) and Macrophage (N=8) Log2 Fold Change for differentially expressed genes (B).

nosuppressive molecule IL10 was upregulated, as well as expression of chemokines associated with poor overall survival and recurrence of nonmetastatic ccRCC, namely CXCL1 [27] and CCL2 (MIP2) [18, 26]. Additionally, we noted increased expression of VEGFA, a potent inducer of angiogenesis, and SPP1 (osteopontin), which in addition to helping osteoclasts bind hydroxyapatite in bone, reportedly functions as a cytokine upregulating IFN-y and IL-12 production [14]. Additionally, TAMs upregulated several key chemotactic and inflammatory signaling receptors including CCR5, CXCR4, IL1R1, ILR2 and IL7R.

TAMs are likely signaling through NF-kB, however regulatory factors may be limiting this signaling

As transcription factors (TF) play a direct role in driving transcription of specific genes, we then investigated which TF may be active in these populations. We identified increased expression of several critical factors involved in NF-kB mediated signaling in TAMs including NFkB subunits: REL, NFKB1 (p50) and NFKB2 (p52). Similarly upregulated were RIPK2, a strong activator of NF-kb that is known to play a role in both innate and adaptive immune responses as well as drive apoptosis, and Caspase 8 which, as a zymogen, induces NF-kB nuclear translocation in immune cells in response to stimulation and in its cleaved form acts in the apoptotic pathway. We also observed increased expression of NFATC2, a pro-inflammatory transcription factor with a REL homology region similar to NFkB subunits. RRAD, a gene reportedly induced by NFkb was similarly upregulated. On the other hand, TANK and TNFAIP3 both of which inhibit activation of NFkB signaling, as well as SMAD2 and SMAD3, both of which are part of the anti-inflammatory response in macrophages were among the upregulated TF. Interestingly, expression of anti-apoptotic BCL2 was increased in TAMs.

TAMs differentially express genes generically associated with the innate immune system

The differential analysis provided several additional genes of interest which were upregulated in TAMs, which did not distinctly belong to the groups described above. These genes include three members of the complement system (C1QA, C1QB and C3) as well as ADA (adenosine deaminase) which cleaves the lymphotoxic deoxyadenosine generated from DNA breakdown, NLRP3, CTSL (cathepsin L), PTGS2 (COX2), MAPK8, and DUSP4. NLRP3 inflammasome has been associated with M2-polarization of macrophages. Although MAPK8 was upregulated, DUSP4 which deactivates members of MAPK pathway through dephosphorylation, also had upregulated expression.

Discussion

Macrophages are a plastic innate cell type that are capable of responding to and modulating a large number of unique environments. Two polarization states have been explored extensively; namely the classically activated pro-inflammatory M1 macrophage, and the alternatively activated immunosuppressive M2 macrophage. However, recent work has identified 17 unique macrophage polarization statuses within the tumor microenvironment (TME) [19], with even more likely to be identified in the future. Our data support a role for a heterogeneous population of macrophages in the TME of human clear cell renal cell carcinoma (ccRCC) that do not fit simply within the traditional M1-M2 paradigm.

These TAMs are transcriptionally unique when compared to circulating monocytes FACS sorted on the same surface receptors; for example, the TAMs express much higher levels of cellular adhesion molecules, which is to be anticipated from a population of cells infiltrating the tumor microenvironment. However, despite increased chemokine, cytokine and interleukin pathway scores, the TAM population had no difference in scores for antigen-processing and cytotoxicity, indicating that these cells are likely not directly stimulating T cells or directly killing cancer cells.

They also expressed some expected molecules which are associated with immunosuppressive macrophages (M2-TAMs), including FN1 which has been shown to have a positive correlation

with CD163 expression [21], the suppressive cytokine IL-10 [21], the macrophage scavenger receptor MSR1 (CD204) and iron uptake receptor TFRC. Interestingly, our data also indicate expression of HAVCR2 (TIM3) on ccRCC intratumoral macrophages, which corroborate other studies which have shown expression of HAVCR2 (TIM3) on ccRCC TAMs is correlated with a shorter progression free survival, increased proliferation of cancer cells, as well as increased resistance to Rapamycin and Sunitnib [17]. This is of particular interest, as TIM3 is most commonly referred to in the context of lymphocytes, and is known to be a late stage suppressive receptor on T-cells. This may be an important factor to consider in studies investigating the effect of agonistic or antagonistic TIM-3 antibodies on tumor infiltrating immune cells.

Besides M2 markers, the TAM population expressed both CD80 and CD40 which are crucially involved with activation of T cells and APCs, as well as CXCL2, CXCL9, CXCL11, CCL4 (MIP1B), CCL20 (MIP3A), which are commonly associated with trafficking of inflammatory immune cells to the site of inflammation. Despite this, the TAMs were also expressing IL-10, which has been well characterized as a suppressive cytokine, as well as both CXCL1 [27] and CCL2 [18, 26], which have been associated with poor overall survival and recurrence of disease in non-metastatic ccRCC. The argument for a partially inflammatory TAM is further corroborated by additional data indicating that these cells are expressing RNA transcripts for several members of the NF-kB family, as NF-kB signaling in macrophages is well established as pro-inflammatory. These findings indicate that the TAM population found in the TME is not solely providing immunosuppressive signaling, however any anti-tumor response caused by increasing the inflammatory cell compartment of the TME is still limited. A study using single cell RNA-seq in non-small cell lung cancer (NSCLC) confirmed that myeloid cells exist in various states of differentiation and branch from monocytes towards M1 or M2 TAMs. Those data are in agreement with ours, indicating that myeloid cells differentiating towards M1 will express CXCL2 and IL-1B, and myeloid cells differentiating towards M2 will express MRC1(CD206) [15]. Our data indicated expression of a mix of M1 and M2 molecules, which is likely due to the heterogeneous nature of the TME of ccRCC and that our analysis was based on bulk sorted TAMs, not scRNA seq.

Our data also indicate production of Complement factors (C1QA, C1QB, C3) by TAMs, which is supported by other groups as well. We saw an increase in C1QA and C1QB, which has a negative prognostic effect in lung adenocarcinoma and ccRCC [24], and has been seen to promote angiogenesis and immunosuppression; additionally, C1Q+ expression positively correlates with $CD163^{+}$ expression on macrophages, indicating that it is being expressed by M2-TAMs [20]. These data highlight the multifaceted effect that TAMs can have in the TME, and supports their value as a therapeutic target.

Collectively, these data display a heterogeneous role for macrophages infiltrating early localized human ccRCC, and strongly support the understanding that the TAM population in ccRCC are not homogenously immunosuppressive. With appropriate immunomodulation, TAMs in the ccRCC TME likely have the potential to drive a more potent anti-tumor response, especially in the context of combination with checkpoint blockade.

Acknowledgements

Funding for this study was generously provided by Dr. Mohamad E. Allaf, the BMS International Immuno-Oncology Network (IIoN) Foundation and the Johns Hopkins University Sidney Kimmel Comprehensive Cancer Center (SKCCC) Cancer Center Support Grant (CCSG) P30CA006973. The authors would like to acknowledge Debebe Theodros and Fan Shen for their careful review of this manuscript.

Disclosure of conflict of interest

None.

Address correspondence to: Dr. Jelani C Zarif, The Johns Hopkins University School of Medicine, The Bunting-Blaustein Cancer Research Building, 1650 Orleans Street-1M45, Baltimore, MD 21231, USA. Tel: 1(410) 502-7885; E-mail: jzarif1@jhmi.edu

References

[1] Nabi S, Kessler ER, Bernard B, Flaig TW and Lam ET. Renal cell carcinoma: a review of biol-

ogy and pathophysiology. F1000Research 2018; 7: 307.
[2] Rossi SH, Klatte T, Usher-Smith J and Stewart GD. Epidemiology and screening for renal cancer. World J Urol 2018; 36: 1341-53.
[3] Rini BI, Campbell SC, Escudier B and Roussy IG. Renal cell carcinoma. Lancet 2009; 373: 1119-32.
[4] Azoury S, Straughan D and Shukla V. Immune checkpoint inhibitors for cancer therapy: clinical efficacy and safety. Curr Cancer Drug Targets 2015; 15: 452-62.
[5] Brahmer JR, Tykodi SS, Chow LQ, Hwu WJ, Topalian SL, Hwu P, Drake CG, Camacho LH, Kauh J, Odunsi K, Pitot HC, Hamid O, Bhatia S, Martins R, Eaton K, Chen S, Salay TM, Alaparthy S, Grosso JF, Korman AJ, Parker SM, Agrawal S, Goldberg SM, Pardoll DM, Gupta A and Wigginton JM. Safety and activity of anti-PD-L1 antibody in patients with advanced cancer. N Engl J Med 2012; 366: 2455-65.
[6] Sharma P. The future of immune checkpoint therapy. Science 2014; 348: 56-51.
[7] Wolchok JD, Chiarion-Sileni V, Gonzalez R, Rutkowski P, Grob JJ, Cowey CL, et al. Overall survival with combined nivolumab and ipilimumab in advanced melanoma. N Engl J Med 2017; NEJMoa1709684.
[8] Daurkin I, Eruslanov E, Stoffs T, Perrin GQ, Algood C, Gilbert SM, Rosser CJ, Su LM, Vieweg J and Kusmartsev S. Tumor-associated macrophages mediate immunosuppression in the renal cancer microenvironment by activating the 15-lipoxygenase-2 pathway. Cancer Res 2011; 71: 6400-9.
[9] Genard G, Lucas S and Michiels C. Reprogramming of tumor-associated macrophages with anticancer therapies: radiotherapy versus chemo- and immunotherapies. Front Immunol 2017; 8: 828.
[10] Quatromoni JG and Eruslanov E. Tumor-associated macrophages: function, phenotype, and link to prognosis in human lung cancer. Am J Transl Res 2012; 4: 376-89.
[11] Noy R and Pollard JW. Tumor-associated macrophages: from mechanisms to therapy. Immunity 2014; 41: 49-61.
[12] Gu J, Johns A, Morser J, Dole WP, Greaves DR and Deng GG. Urokinase plasminogen activator receptor promotes macrophage infiltration into the vascular wall of ApoE deficient mice. J Cell Physiol 2005; 204: 73-82.
[13] Flecken T and Sarobe P. Tim-3 expression in tumour-associated macrophages: a new player in HCC progression. Gut 2015; 64: 1502-3.
[14] Zhang Y, Du W, Chen Z and Xiang C. Upregulation of PD-L1 by SPP1 mediates macrophage polarization and facilitates immune escape in lung adenocarcinoma. Exp Cell Res 2017; 359: 449-57.
[15] Song Q, Hawkins GA, Wudel L, Chou PC, Forbes E, Pullikuth AK, Liu L, Jin G, Craddock L, Topaloglu U, Kucera G, O'Neill S, Levine EA, Sun P, Watabe K, Lu Y, Alexander-Miller MA, Pasche B, Miller LD and Zhang W. Dissecting intratumoral myeloid cell plasticity by single cell RNA-seq. Cancer Med 2019; 8: 3072-85.
[16] Janzen NK, Kim HL, Figlin RA and Belldegrun AS. Surveillance after radical or partial nephrectomy for localized renal cell carcinoma and management of recurrent disease. Urol Clin North Am 2003; 30: 843-52.
[17] Komohara Y, Morita T, Annan DA, Horlad H, Ohnishi K, Yamada S, Nakayama T, Kitada S, Suzu S, Kinoshita I, Dosaka-Akita H, Akashi K, Takeya M and Jinushi M. The coordinated actions of TIM-3 on cancer and myeloid cells in the regulation of tumorigenicity and clinical prognosis in clear cell renal cell carcinomas. Cancer Immunol Res 2015; 3: 999-1007.
[18] Wang Z, Xie H, Zhou L, Liu Z, Fu H, Zhu Y, Xu L and Xu J. CCL2/CCR2 axis is associated with postoperative survival and recurrence of patients with non-metastatic clear-cell renal cell carcinoma. Oncotarget 2016; 7: 51525-51534.
[19] Chevrier S, Levine JH, Zanotelli VRT, Silina K, Schulz D, Bacac M, Ries CH, Ailles L, Jewett MAS, Moch H, van den Broek M, Beisel C, Stadler MB, Gedye C, Reis B, Pe'er D and Bodenmiller B. An immune atlas of clear cell renal cell carcinoma. Cell 2017; 169: 736-749, e18.
[20] Roumenina LT, Daugan MV, Noé R, Petitprez F, Vano YA, Sanchez-Salas R, Becht E, Meilleroux J, Clec'h BL, Giraldo NA, Merle NS, Sun CM, Verkarre V, Validire P, Selves J, Lacroix L, Delfour O, Vandenberghe I, Thuilliez C, Keddani S, Sakhi IB, Barret E, Ferré P, Corvaïa N, Passioukov A, Chetaille E, Botto M, de Reynies A, Oudard SM, Mejean A, Cathelineau X, Sautès-Fridman C and Fridman WH. Tumor cells hijack macrophage-produced complement C1q to promote tumor growth. Cancer Immunol Res 2019; 7: 1091-1105.
[21] Dannenmann SR, Thielicke J, Stöckli M, Matter C, von Boehmer L, Cecconi V, Hermanns T, Hefermehl L, Schraml P, Moch H, Knuth A and van den Broek M. Tumor-associated macrophages subvert t-cell function and correlate with reduced survival in clear cell renal cell carcinoma. OncoImmunology 2013; 2: e23562.
[22] Chittezhath M, Dhillon MK, Lim JY, Laoui D, Shalova IN, Teo YL and Biswas SK. Molecular profiling reveals a tumor-promoting phenotype of monocytes and macrophages in human cancer progression. Immunity 014; 41: 815-829.
[23] Komohara Y, Hasita H, Ohnishi K, Fujiwara Y, Suzu S, Eto M and Takeya M. Macrophage infil-

tration and its prognostic relevance in clear cell renal cell carcinoma. Cancer Sci 2011; 102: 1424-1431.

[24] Mangogna A, Agostinis C, Bonazza D, Belmonte B, Zacchi P, Zito G, Romano A, Zanconati F, Ricci G, Kishore U and Bulla R. Is the complement protein C1q a Pro- or anti-tumorigenic factor? Bioinformatics analysis involving human carcinomas. Front Immunol 2019; 10: 865.

[25] Petrella BL and Vincenti MP. Interleukin-1β mediates metalloproteinase-dependent renal cell carcinoma tumor cell invasion through the activation of CCAAT enhancer binding protein β. Cancer Med 2012; 1: 17-27.

[26] Yang Y, Zhai C, Chang Y, Zhou L, Shi T, Tan C, Xu L and Xu J. High expression of chemokine CCL2 is associated with recurrence after surgery in clear-cell renal cell carcinoma. Urol Oncol 2016; 34: 238, e19-26.

[27] Tan W, Hildebrandt MA, Pu X, Huang M, Lin J, Matin SF, Tamboli P, Wood CG and Wu X. Role of inflammatory related gene expression in clear cell renal cell carcinoma development and clinical outcomes. J Urol 2011; 186: 2071-7.

Supplementary Table 1. Monocyte and Macrophage pathway scores and significance

	PBMC Monocyte							Tumor TAM									
	Sample 1	Sample 2	Sample 4	Sample 5	Sample 6	Sample 7	Sample 8	Sample 1	Sample 2	Sample 3	Sample 4	Sample 5	Sample 6	Sample 7	Sample 8	*P*-value	Asterisks
Adhesion	-1.0558	-1.1075	-1.4722	-2.5805	-1.3310	-1.6665	-2.7233	1.8118	1.3656	0.7034	0.3974	1.2242	0.8501	1.4421	4.1421	0.0003	***
Antigen Processing	1.3941	-0.9404	2.2201	-2.5763	-1.6186	0.6180	-0.2640	3.2933	0.2903	-1.4694	1.0259	-0.9741	-0.9864	-0.8631	0.8507	0.8665	NS
B-Cell Functions	-1.3269	0.0729	-1.3600	-1.7395	-1.5934	-1.0021	-1.3989	0.9962	2.2389	1.3469	0.2803	0.6312	-0.2887	0.7839	2.3594	0.0006	***
Cell Cycle	-0.9866	-1.9289	-0.4710	-2.0703	-2.5522	-1.2858	-0.9698	1.6875	1.4784	1.4947	-0.4209	1.7464	1.1728	0.4946	2.6111	0.0003	***
Cell Functions	-1.3873	-2.2132	-1.6915	-1.0335	-2.8186	-0.6580	-4.7132	1.7577	1.5950	1.2140	0.8685	1.0351	1.1991	2.2192	4.6265	0.0003	***
Chemokines	-3.0916	0.0483	-3.6167	-5.6430	-3.3137	-1.4837	-5.7379	2.3189	4.3454	3.1289	2.1041	2.2490	3.2177	1.5176	3.9568	0.0003	***
Cytokines	-3.0177	-0.0432	-4.1333	-5.0591	-2.9709	-0.6737	-3.6281	3.1075	3.4547	2.3399	-0.3614	2.2355	3.0996	0.5654	5.0850	0.0006	***
Cytotoxicity	-0.8177	-0.2629	0.6824	-0.6454	0.1653	1.4981	1.8354	0.7701	-0.5162	-1.5511	-0.8626	-0.8928	-0.4730	-0.5009	1.5713	0.2319	NS
Interleukins	-1.8663	2.3024	-2.9319	-4.2052	-3.1295	-1.3276	-3.4415	1.6879	2.4874	2.5988	0.0576	1.8014	2.3689	0.4498	3.1476	0.0037	**
Macrophage Functions	-1.2108	-0.8132	-0.6709	-1.5883	-1.5562	-1.0334	-1.6055	0.6783	2.0574	1.2041	0.0222	1.0221	-0.1263	0.3050	3.3154	0.0003	***
NK Cell Functions	-0.0979	-0.0460	-0.9773	-0.9133	-0.6760	-2.2328	-2.5874	0.2731	2.2745	-0.3817	1.3066	0.7216	1.3824	0.6385	1.3158	0.0012	**
Pathogen Defense	-1.5720	1.3026	-1.5992	-3.2375	-0.9933	0.2439	-1.5532	2.2687	1.3128	0.6544	-0.2925	0.2558	1.3215	-0.1584	2.0466	0.0093	**
Regulation	-3.0260	-1.2138	-3.4330	-6.2974	-4.3839	-3.3938	-6.2514	3.5748	4.8340	3.1101	1.4933	4.0083	2.2227	2.3823	6.3738	0.0003	***
Senescence	-2.3141	-0.4213	-1.5132	-1.9636	-1.6057	-1.7148	-1.7185	-0.0811	2.2419	1.3659	0.7293	1.2969	1.9690	0.9321	2.7970	0.0003	***
T-Cell Functions	-2.2610	-1.0323	-2.4822	-4.1559	-2.9366	-0.1883	-2.8269	2.4046	3.8089	1.9163	0.6983	0.8491	0.8640	1.5177	3.8242	0.0003	***
TLR	0.8058	-0.7034	0.6983	1.1861	0.2070	0.6505	0.1114	-0.0198	0.5821	-0.4519	-1.4334	-1.5281	-0.1718	-2.5368	2.6040	0.0939	NS
TNF Superfamily	-2.1029	-0.3065	-2.0721	-3.2043	-1.4361	-1.6322	-0.6035	0.1752	1.3875	1.5592	0.2849	1.5877	1.3134	0.9862	4.0634	0.0003	***
Transporter Functions	-0.7342	-0.4820	-0.3050	-0.6891	0.5932	0.6318	2.2697	0.4090	0.0587	-0.9276	-2.5508	-1.5788	1.5360	-2.4398	4.2089	0.4634	NS

Supplementary Table 2. Monocyte and Macrophage normalized absolute gene expression levels and significance

	PBMC Monocyte							Tumor TAM									
Probe Name	Sample 1	Sample 2	Sample 4	Sample 5	Sample 6	Sample 7	Sample 8	Sample 1	Sample 2	Sample 3	Sample 4	Sample 5	Sample 6	Sample 7	Sample 8	*P*-Value	Aterisk
CXCR4	61531.39	12199.32	41868.19	34865.9	27862.19	56974.68	32859.38	100709.29	130051.44	92411.95	79525.76	70051.43	49654.31	86872.96	134298.58	0.0429	*
IL1B	11058.84	46640.93	11309.56	2732.56	6394.84	9100.23	4036.34	52409.08	72597.88	49989.59	18024.8	31804.07	45976.52	18692.78	109931.34	0.0365	*
ICAM1	9122.28	14217.88	2367.91	2958.06	5790.98	13609.03	4079.67	35518.45	37564.26	29229.46	17102.38	18603.96	23531.5	17203.73	44857.86	0.0303	*
CXCL2	4069.52	15496.82	1241.23	950.72	408.09	1477.07	100	21195.86	37071.97	15110.02	9980.32	15098.25	19020.58	9455.59	53157.34	0.0303	*
PLAUR	4530.6	3466.1	1332.88	979.67	3705.98	1479.57	1407.34	10423.04	21154.61	11288.57	7471.48	8425.3	15854.22	6714	39643.85	0.00462	**
TNFAIP3	3782.09	9320.57	978.24	662	1667.59	708.49	1681.23	7986.32	11874.26	8287.75	7586.08	8653.96	10236.78	6962.58	17435.31	0.0227	*
TLR2	3027.59	3762.49	3766.53	3453.99	3562.01	5582.81	3396.5	9697.49	7708.58	7303	6456.93	8477.22	10175.5	9737.96	15453.68	0.0305	*
NFKB1	1647.93	2973.01	828.82	1503.02	1341.32	2440.91	1582.97	7372.59	9563.07	13584	2312.23	6212.64	6866.55	4534.73	23696.65	0.0107	*
THBS1	675.46	229.32	318.78	100	100	100	169.44	6523.5	2166.86	8776.64	475.25	6544.14	11648.5	2117.73	24766.57	0.00126	**
C1QB	3579.69	100	371.57	959.1	100	100	100	6423.38	6053.78	5524.39	18669.71	11620.49	816.63	13722.44	100	0.0408	*
PTGS2	2461.11	5478.32	2794.27	957.58	893.87	2420.89	823.21	10841.73	11344.41	8436.75	5803.04	5095.32	4210.43	2921.39	13596.37	0.0327	*
TANK	2560.51	3777.9	2111.89	2990.81	1955.53	1699.88	1543.51	8696.27	9300.12	5530.21	2638.05	3518.7	7125.79	2347	21262.94	0.026	*
CCL4	287.43	16010.75	100	100	135.69	100	100	6610.62	9535.39	4448.85	5292.95	6191.67	4867.98	2566.62	9290.29	0.0217	*
REL	1744.93	2878.75	629.58	1097.75	1031.63	1339.37	464.21	5550.9	5688.02	6944.49	3807.65	3969.02	3167.54	3622.47	9350.57	0.00772	**
CD58	1443.13	1998.62	2636.87	3576.63	1493.58	605.85	1999.99	6016.4	4438.51	4560.59	1176.34	4603.06	2026.85	2759.69	9960.88	0.0408	*
SPP1	100	100	100	100	100	100	100	100	1656.78	980.1	3124.54	100	1058.2	20874.46	2030.6	0.000457	***
SMAD3	1211.99	466.8	685.37	634.58	629.75	100	644.48	7143.74	6435.35	1695.96	797.71	1236.14	758.89	1915.01	9286.52	0.0103	*
CD40	3227.59	414.23	227.13	817.41	1175.6	761.06	680.85	2657.77	7396.21	2337.33	3006.57	1371.93	2247.21	2910.53	4490.68	0.0231	*
FN1	100	100	100	358.81	100	100	100	557.82	2208.38	1242	6840.06	775.83	1280.92	6477.49	6886.72	0.000457	***
MSR1	1852.72	206.66	1178.47	845.59	100	100	100	1742.38	5448.79	2740.08	4237.96	2245.62	650.48	3738.31	2252.88	0.0324	*
CCL20	100	1699.51	100	100	100	100	100	148.23	3552.79	6156.45	575.25	1800.29	5842.52	888.12	3669.4	0.0227	*
BCL2	657.49	177.66	1067.9	754.94	319.02	320.45	1643.32	1126.04	5211.55	1705.28	1835.85	2086.85	1338.66	3433.02	5711.31	0.025	*
VEGFA	119.76	100	100	310.05	239.26	816.14	100	3367.73	5620.8	3088.12	2316.72	1938.08	1910.19	2389.24	945.61	0.00533	**
SMAD2	956.9	464.99	566.82	433.46	1481.15	100	100	3393.73	838.28	271.21	917.92	100	1669.8	995.52	12127.11	0.0408	*
A2M	100	100	100	100	100	100	100	100	4377.23	1039.46	3459.35	1060.4	639.87	5451.81	3514.94	0.000457	***
NLRP3	449.11	1677.76	436.32	100	562.42	1036.45	525.34	1638.35	3060.5	3004.31	662.88	2700.93	2350.91	1671.26	2995.04	0.0498	*
ITGAX	1227.56	501.24	362.61	246.06	466.1	580.81	177.95	2971.14	2625.54	4155.52	1050.5	1010.48	2066.92	2419.41	1066.16	0.00505	**
C1QA	1600.02	303.65	100	326.05	100	100	100	863.39	3058.52	2738.92	4240.21	2660.99	216.83	3372.69	100	0.0303	*
HAVCR2	347.31	171.31	500.08	289.48	641.14	327.96	100	388.78	1812.97	2110.35	2352.67	726.9	1977.36	1901.74	5707.54	0.00533	**
CTSL	772.47	100	533.95	499.74	215.44	100	318.76	910.2	2313.17	741.47	1223.53	813.77	2031.56	3803.47	4648.91	0.00533	**
CCR5	566.47	484.02	272.95	431.18	175.04	533.25	311.02	2701.98	4432.58	1666.86	1406.66	576.13	494.93	1037.75	3620.43	0.0122	*
THBD	137.73	100	100	100	100	100	100	808.77	1805.06	2458.39	123.59	644.03	1458.86	714.36	5221.55	0.0024	**
RIPK2	1143.73	1640.59	834.79	294.05	763.36	500.7	312.57	3084.26	2046.26	1331.63	2284.14	1133.29	1098.27	1257.37	843.89	0.0365	*
DUSP4	100	100	100	100	100	100	100	2699.38	3299.72	3559.54	613.45	534.19	263.96	1102.91	100	0.00168	**
IL18	1225.17	711.53	221.15	851.69	422.59	498.2	141.59	334.17	2625.54	970.78	1378.57	942.58	1118.3	1613.34	1525.78	0.0408	*
CXCL1	100	164.97	100	100	259.98	100	100	367.98	2004.75	556.4	503.34	333.5	1901.94	1531.28	1717.91	0.00316	**
PLAU	100	100	100	100	100	100	100	293.86	3558.72	731	1620.13	665	332.31	1462.5	100	0.0024	**

CLEC5A	726.96	100	100	100	259.98	100	100	656.64	1128.9	1343.27	871.86	141.79	814.28	1476.98	1966.56	0.0212	*
IL1R1	100	100	100	100	100	100	100	100	359.83	846.24	100	1017.47	655.19	596.1	4004.7	0.0024	**
ADA	586.83	454.11	376.55	362.62	218.55	332.97	301.74	980.41	1366.15	827.61	269.65	389.41	943.9	1018.44	1424.06	0.0327	*
TFRC	131.74	171.31	183.3	201.88	123.26	100	100	352.38	100	838.09	910.06	1471.78	312.28	698.67	2124.79	0.00533	**
ALCAM	323.36	177.66	137.47	100	263.09	100	100	806.17	199.68	178.09	419.08	506.24	100	587.66	3187.18	0.0384	*
C3	100	100	100	100	100	100	100	100	1700.28	264.23	1604.4	100	100	1773.83	100	0.00533	**
NFATC2	100	100	263.99	100	168.83	100	100	1024.62	648.48	373.65	805.57	743.88	603.34	993.1	100	0.00533	**
IL7R	132.94	100	100	100	162.62	100	100	100	1708.19	533.12	199.99	239.64	100	181	1695.31	0.0384	*
IL1R2	100	100	100	100	100	100	100	218.45	316.33	100	100	307.54	810.74	100	2689.89	0.00736	**
CXCL11	100	100	100	100	100	100	100	230.15	2720.44	100	1146	100	100	100	100	0.0437	*
RRAD	100	100	100	100	100	100	100	244.45	579.28	253.75	276.39	100	453.68	225.65	2456.31	0.0147	*
NFKB2	100	190.35	100	100	136.72	100	100	327.67	251.09	126.88	100	184.72	266.32	100	2546.73	0.0365	*
ITGA6	192.82	100	100	100	100	100	100	100	100	100	361.78	100	100	368.04	2335.76	0.031	*
IL10	100	100	100	100	100	100	100	100	850.14	728.67	211.22	100	972.18	243.75	100	0.00462	**
AXL	100	100	144.45	100	100	100	100	141.73	733.49	180.42	383.12	429.35	100	619.03	100	0.0107	*
MAPK8	100	100	100	100	100	100	100	200.24	100	100	100	482.27	100	100	1224.39	0.0408	*
CASP8	2812.02	503.96	1176.48	1391.04	1024.38	610.85	1605.41	100	415.18	199.05	450.54	283.57	532.64	252.2	100	0.0415	*
CXCL9	100	100	100	100	100	100	100	618.93	421.12	171.11	387.62	120.82	168.51	183.42	100	0.00533	**
ICAM4	100	100	100	100	100	100	100	100	369.71	187.41	100	184.72	100	100	828.82	0.0498	*
CD80	100	100	100	100	100	100	100	100	100	167.62	261.78	143.78	100	100	621.61	0.0365	*
CD9	100	115.11	100	100	119.11	100	100	100	421.12	152.49	253.92	100	100	353.56	100	0.0327	*

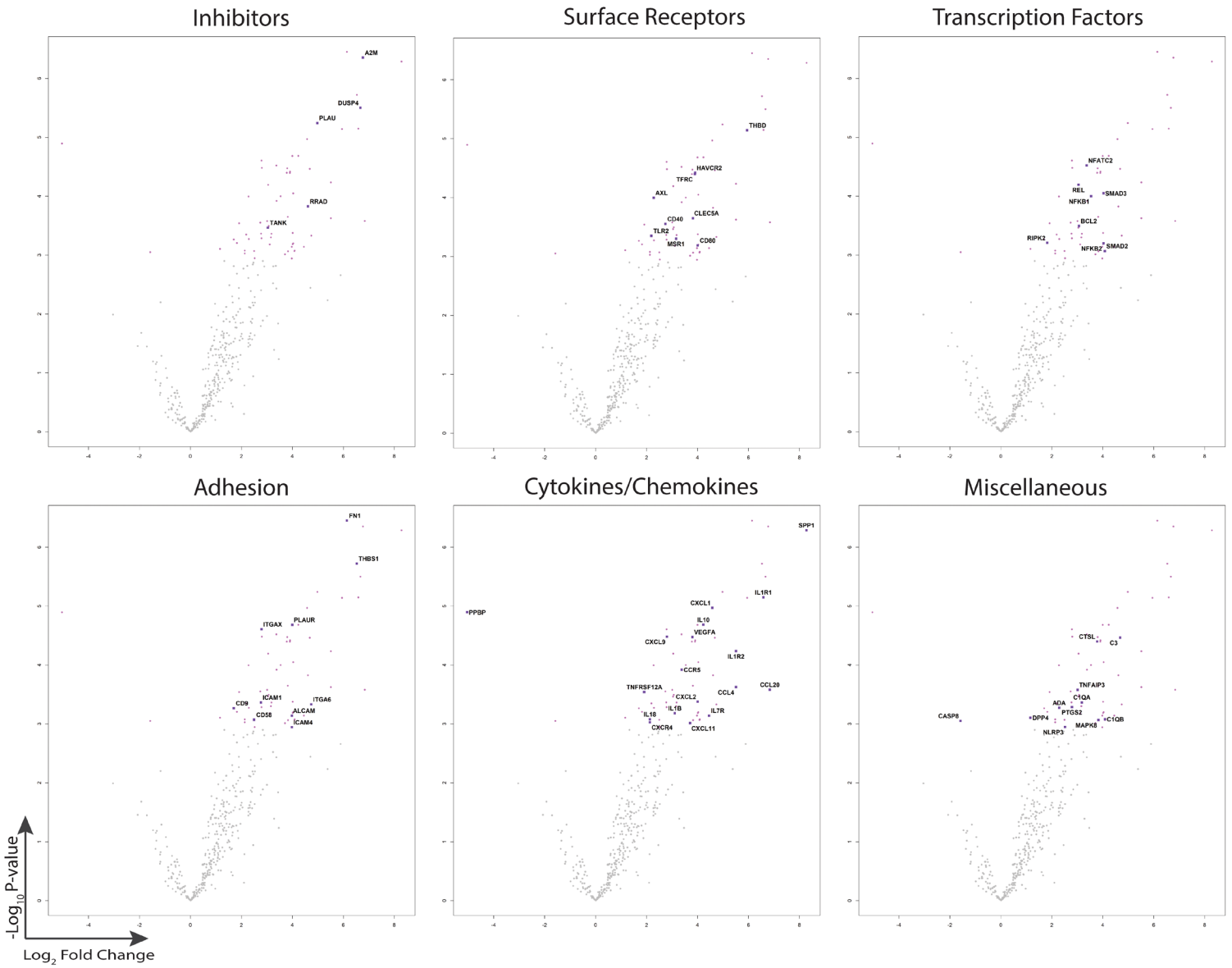

Supplementary Figure 1. Macrophage differentially expressed genes. Macrophage (N=8) Log2 Fold Change for differentially expressed genes represented by gene classification grouping.